Earth and Planetary Science Letters 292 (2010) 231–237

Contents lists available at ScienceDirect

Earth and Planetary Science Letters

journal homepage: www.elsevier.com/locate/epsl

# Astronomical tuning of the Cenomanian Scaglia Bianca Formation at Furlo, Italy

Luca Lanci [a,c,*], Giovanni Muttoni [b,c], Elisabetta Erba [b]

[a] DIGEOTECA, University of Urbino, Campus Scientifico SOGESTA, 61100, Urbino (PU), Italy
[b] Dipartimento di Scienze della Terra "A.Desio", Università degli Studi di Milano, Via Mangiagalli 34, 20133 Milano, Italy
[c] ALP — Alpine Laboratory of Paleomagnetism, via Madonna dei Boschi 76, 12016 Peveragno (CN), Italy

ARTICLE INFO

*Article history:*
Received 30 August 2009
Received in revised form 26 January 2010
Accepted 26 January 2010
Available online 16 February 2010

Editor: P. DeMenocal

*Keywords:*
Cenomanian
black shales
Bonarelli Level
rock magnetism
cyclostratigraphy

ABSTRACT

The astronomical tuning of the upper Cenomanian rhythmic succession of marine limestones and black shales that prelude to the Bonarelli Level (=Oceanic Anoxic Event 2) in the classic Furlo section of central Italy was achieved using cyclostratigraphic analyses on environmentally controlled rock-magnetic properties and the $CaCO_3$ content of the limestones. The astronomical tuning was based on the stable 405 kyr-long eccentricity cycle observed in the rock-magnetic record and correlated to the orbital solution of Laskar et al. (2004), and the phase relationship was established by the eccentricity-modulated precession signal observed in the $CaCO_3$ record. According to our tuning, pre-Bonarelli black shales formed during eccentricity minima and reduced seasonality when reduced deep-water circulation (sea bottom ventilation) in a paleogeographically constricted Alpine Tethys–Central Atlantic Ocean promoted organic matter preservation and possibly a reduced carbonate dissolution resulting in a higher sedimentation rate. In compliance, the onset of the OAE2 at Furlo corresponds to the eccentricity minimum nominally placed at 93.92 Ma, with the full development of OAE2 persisting much longer than any black shale precursor across at least one long eccentricity maximum.



## 1. Introduction

In the Furlo Gorge of central Italy (Fig. 1a), the Bonarelli Level is exposed at the top of a 20 m-thick section of upper Cenomanian limestones and black shales pertaining to the Scaglia Bianca Formation. It represents the local sedimentary expression of Oceanic Anoxic Event (OAE) 2 (e.g., Arthur and Premoli Silva, 1982), and the associated $\delta^{13}C_{org}$ positive excursion (e.g., Tsikos et al., 2004; Kuroda et al., 2007; Mort et al., 2007) (Fig. 2). Black shale deposition across the OAE2 appears global in nature as it was recognized in all main oceanic basins (Arthur et al., 1990). Furthermore, the record from the nearby Abruzzi platform shows that the Bonarelli Level corresponds to a phase of fast sea-level rise (drawn platform) that was correlated worldwide and related to climate changes (Galeotti et al., 2009).

Rhythmic episodes of organic matter accumulation resulting in the deposition of thin black shale layers occur below the Bonarelli Level (Coccioni and Galeotti, 2003). Pre-Bonarelli black shales of Cenomanian age seem to be a regional feature of the Alpine Tethys Ocean and the adjacent Central Atlantic Ocean (Italian Apennines as well as Deep Sea Drilling Project and Ocean Drilling Program sites in the Iberia abyssal plain, Galicia margin, Newfoundland basin, Blake Nose, Demerara rise, and Cape Verde basin).

Two main models have been proposed to explain the preservation of organic matter within pre-Bonarelli black shales, namely the anti-monsoonal model, originally developed for the Aptian–Albian black shales of the Marne a Fucoidi Fm., which lies immediately below the Scaglia Bianca Fm. (Herbert and Fischer, 1986), and the monsoonal model, developed for Pliocene–Pleistocene Mediterranean sapropels (Rossignol-Strick, 1985; Hilgen, 1991a; Hilgen et al., 1995) and, recently applied to Cenomanian black shales by Mitchell et al. (2008). According to the anti-monsoonal model, black shales were deposited during periods of low orbital forcing leading to reduced seasonal contrast and deep-water formation, and resulting in decreased sea bottom ventilation, deep-intermediate water mass hypoxia and enhanced preservation of organic matter (Herbert and Fischer, 1986).

According to the monsoonal model, Pliocene–Pleistocene sapropels were deposited in the eastern Mediterranean Sea at times of intense (northern) summer monsoons (Rossignol-Strick, 1985) during eccentricity maxima when the seasonal contrast in the Northern Hemisphere — and hence monsoonality — was significantly increased, enhancing flood discharge in the Mediterranean Sea that prevented deep-water formation and promoted anoxia and organic matter preservation (Rohling and Hilgen, 1991; Hilgen, 1991b; Emeis and Weissert, 2009). Though applied to different time intervals and paleogeographic settings, both models deem orbital forcing as a triggering mechanism for deposition of $C_{org}$-rich sediments, but in opposite phase relationships.

Choosing among the possible orbital scenarios (and triggering mechanisms) of Cenomanian black shales formation (i.e., anti-monsoonal versus monsoonal) requires establishing the correct phase relationship

* Corresponding author. Also at School of Earth and Environment, University of Western Australia, 35 Stirling Highway, Crawley WA, 6009, Australia.
*E-mail addresses:* llanci@cyllene.uwa.edu.au, luca.lanci@uniurb.it (L. Lanci).

0012-821X/$ – see front matter © 2010 Elsevier B.V. All rights reserved.
doi:10.1016/j.epsl.2010.01.041

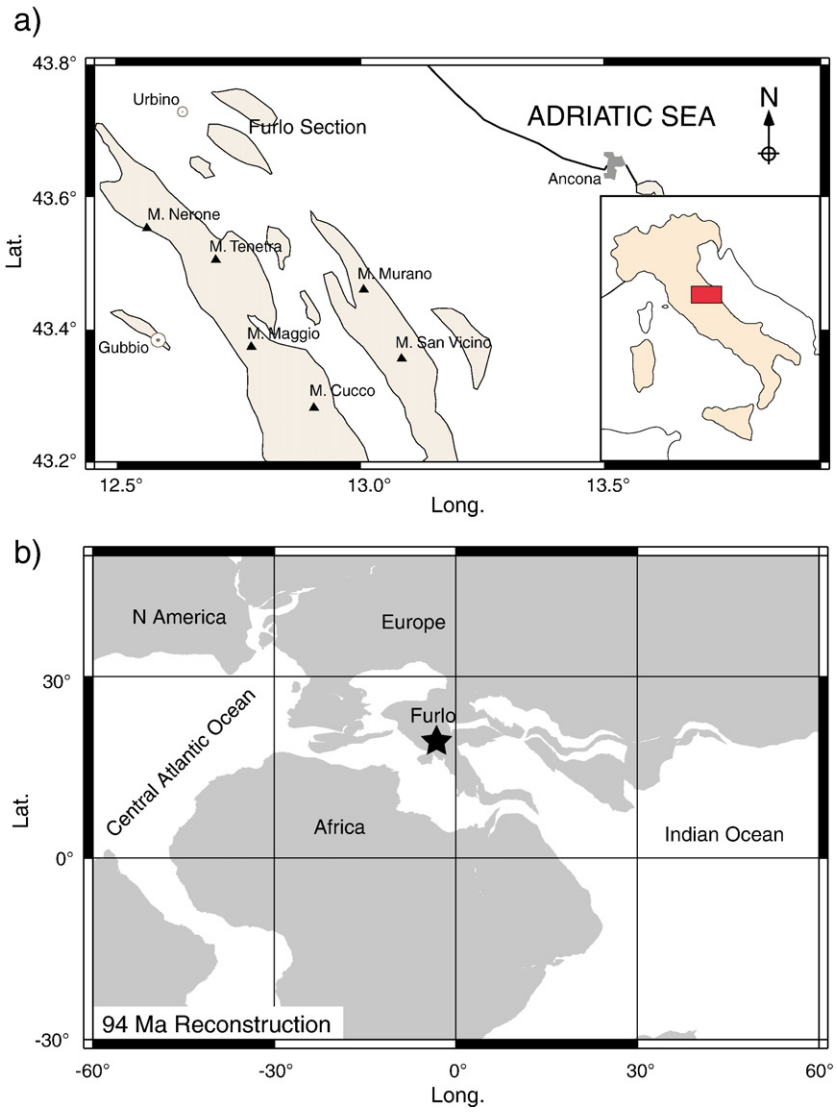


**Fig. 1.** Palaeo-location of the Furlo area and present day location of the studied sections. (a) Geologic sketch map of the central Apennines with location of the Furlo section; the shaded area represents the Mesozoic formation. (b) Paleogeographic map (www.odsn.de) of the Tethys–Central Atlantic region at ~94 Ma (Cenomanian–Turonian boundary) with approximate location of the Furlo section.

between the forcing mechanism (eccentricity) and the periodic signal extracted from the geologic record and related to black shales. Here we present the results of a cyclostratigraphic study performed on a ~2.1 Myr continuous record of rock-magnetic properties and calcium carbonate ($CaCO_3$) content of the Scaglia Bianca Fm. at Furlo. Spectral analysis is also used to determine the orbital conditions at the time of onset of the Bonarelli Level.

## 2. Lithology and age

The Scaglia Bianca Fm. at Furlo (Fig. 1a) was deposited at a latitude of ~20°N in the tropical belt of the Tethys seaway (Fig. 1b). The Furlo section has already been studied by Mitchell et al. (2008) for cyclostratigraphy and by Mort et al. (2007) for organic carbon ($\delta^{13}C_{org}$) stratigraphy across the Bonarelli Level. From base to top, we distinguish the following main stratigraphic intervals relative to the base of the Bonarelli Level placed at meter level 0 (Fig. 2).

(I) The interval from −20 to −18.50 m consists of white to light grey micritic limestones with pinkish chert lenses and nodules.
(II) The interval from −18.50 to −13.30 m consists of couplets of light grey micritic limestones with pinkish to light grey chert layers and lenses, and black shales. Black chert occurs from −16.57 m upwards.
(III) The interval from −13.30 to −3.20 m consists of couplets of light grey micritic limestones with black chert layers, and black shales.
(IV) The interval from −3.20 to 0 m consists of light grey micritic limestones with black chert layers. A single, thin black shale occurs at −0.7 m.
(V) The Bonarelli Level is 1 m-thick (from 0 to +1 m) and consists of couplets of black laminated organic-rich shales, radiolarian-rich layers, and occasional black chert layers.
(VI) The interval from meter level +1 to +4 m consists of light grey micritic limestones with light grey to reddish chert layers.

Calcareous nannofossils are common and moderately well preserved in limestones whereas their abundance and preservation is extremely variable in black shales where they can range from very abundant to scarce and from moderately to poorly preserved. The last occurrence of *Axopodorhadbus albianus* (at −0.63 m) and the first occurrence of *Quadrum gartneri* (at +0.74 m) are used to identify the NC 12** zone (Bralower et al., 1995) of latest Cenomanian age (Fig. 2). The FO of *Q. gartneri* approximates the Cenomanian–Turonian boundary, as calibrated

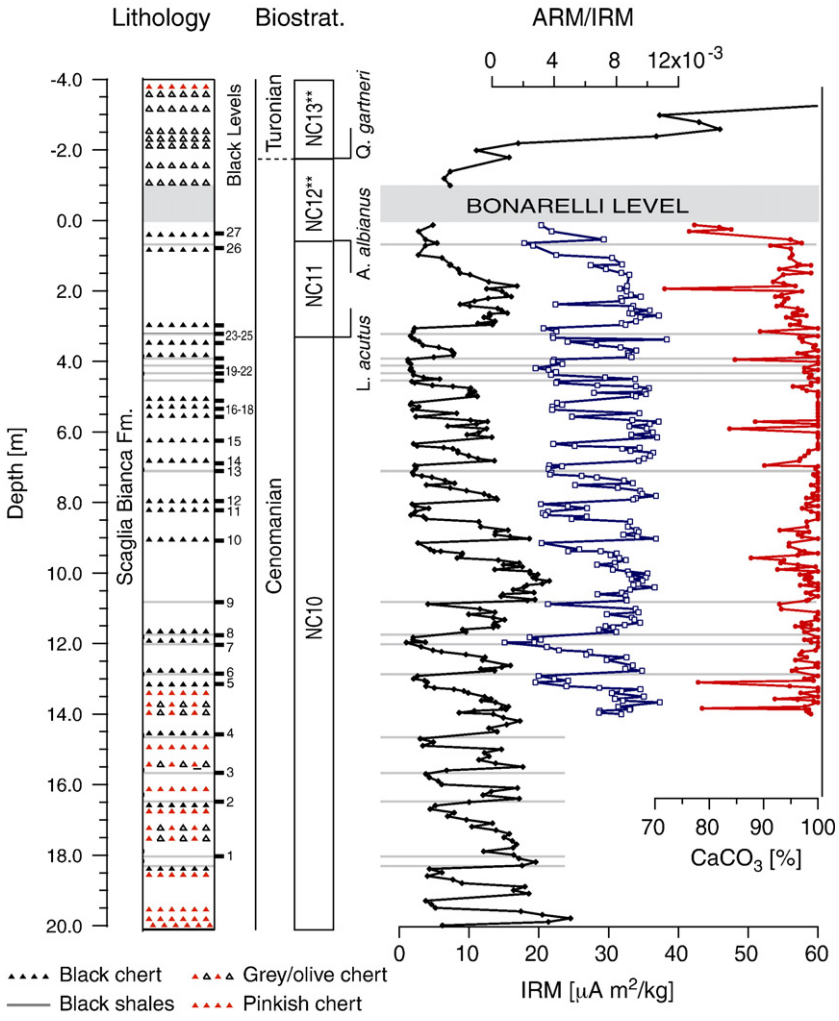


**Fig. 2.** Schematic lithology, nannofossil zonation, rock-magnetic properties and $CaCO_3$ contents of the Furlo section. Grey bands show the black shale levels. The black levels, numbered 1 to 27, are reported accordingly to Mitchell et al. (2008) and references therein, and include black shales and black chert levels.

in other reference sections, including the Pueblo Cenomanian–Turonian boundary stratotype (Tsikos et al., 2004; Voigt et al., 2007). According to planktonic foraminifera biostratigraphy, the Furlo section spans the upper part of the *Rotalipora cushmani* Zone through the lower part of the *Helvetoglobotruncana helvetica* Zone, with the Cenomanian–Turonian boundary approximated by the first occurrence of *H. helvetica* placed 6.50 m above the top of the Bonarelli Level (Mitchell et al., 2008).

## 3. Rock magnetism and cyclostratigraphy

We performed cyclostratigraphic analyses on a rock-magnetic record retrieved from the stratigraphic interval below the Bonarelli Level. The calcareous portion of the Furlo section was sampled with a portable rock drill; a total of 247 specimens were taken in the 20 m below the Bonarelli Level at an average sampling resolution of 1 sample every 8 cm, whereas additional 12 specimens were taken in the 2.8 m above the Bonarelli Level (Fig. 2). The sampling was restrained to the largely dominant limestone beds in order to keep the rock-magnetic record independent from lithological variations.

The magnetic mineralogy of the Scaglia Bianca Fm. consists essentially of detrital magnetite carrying a primary paleomagnetic signal (e.g., Lowrie et al., 1980; Lowrie and Alvarez, 1984). The rock-magnetic properties were studied by measuring the Anhysteretic Remanent Magnetization (ARM), and the Isothermal Remanent Magnetization (IRM) of each sample. The ARM was acquired by applying a peak alternating field of 0.1 T and a bias field of 50 μT, whereas the IRM was acquired in 0.1 and 1 T fields with a pulse magnetizer. All measurements were made on a DC-SQUID 2G cryogenic magnetometer located in a magnetically shielded room at the Alpine Laboratory of Paleomagnetism. The ARM to IRM ratio was computed dividing the ARM intensity by the IRM intensity at 0.1 T field. The IRM intensity is regarded as a proxy of magnetite concentration and the ARM/IRM ratio as a proxy of magnetite grain size, whereby high (low) ARM/IRM values are typical for small single-domain (large multidomain) magnetite grains (e.g., Dunlop and Ozdemir, 1997).

The IRM intensity curve shows an exceptionally clear cyclic pattern (Fig. 2) and the ARM/IRM curve tracks this pattern showing low (high) ARM/IRM values in correspondence of low (high) IRM intensities. Limestones with high IRM and ARM/IRM values are interpreted as enriched in single-domain magnetite relative to limestones with low IRM and ARM/IRM values, which occur during the deposition of black levels. Hence, oxygen levels probably controlled magnetite variability; well-oxygenated bottom waters promoted magnetite preservation whereas poorly oxygenated to euxinic waters promoted instead magnetite dissolution. The rapid increase of the IRM intensity observed above the Bonareli Level (Fig. 2) concurs with the disappearance of the black shales and indicates larger concentrations of magnetic minerals reflecting the end of the euxinic conditions that promoted magnetite dissolution as well as black shale's preservation.

We recognized periodicities in the rock-magnetic record by means of spectral analysis. We applied the Lomb–Scargle algorithm (Press et al., 2002) to compute a simple periodogram of unevenly spaced data in

depth scale; as shown later more sophisticated techniques such as the Multi Taper Method gave virtually identical results. The periodogram of the IRM curve shows three well-defined and large-amplitude peaks corresponding to frequencies of ~0.25 cycle/m, ~0.80 cycle/m and ~1.0 cycle/m (Fig. 3). The IRM periodogram has a striking resemblance with the periodogram of Earth's eccentricity computed from the Laskar et al. (2004) solution for a similar time interval (93–96 Ma) when it is rescaled to a sedimentation rate of 10 m/Myr, which is estimated on the average thickness of the Scaglia Bianca Fm. in the Umbria-Marche basin and the duration of the Cenomanian stage (Gradstein et al., 2004). The ratios between the highly significant IRM peak frequencies, as well as their relative amplitude, match that of the orbital eccentricity (Fig. 3), therefore, we interpret the IRM spectral peaks as Earth's eccentricity cycles of periods ~400 kyr (~0.25 cycle/m), ~125 kyr (~0.8 cycle/m) and ~100 kyr (~1.0 cycle/m).

To establish the correct phase relationship between IRM and eccentricity, we measured the calcium carbonate ($CaCO_3$) content of the 197 limestone samples using standard techniques (Fig. 2). The $CaCO_3$ measurements were interpolated to evenly spaced samples, with an interval equivalent to their average sampling interval of 7 cm, in order to compute the frequency spectrum using the Multi Taper Method according to the algorithm described by Mann and Lees (1996), which was used also for subsequent filtering. The power spectrum (Fig. 4a) is characterized by two statistically significant frequency peaks at ~4 cycles/m and ~5 cycles/m, which correspond to precessional periods of ~25 and ~20 kyr, assuming the average sediment accumulation rate of ~10 m/Myr established above. Evidences of short eccentricity are also found in the $CaCO_3$ spectrum at ~1 cycle/m, this frequency (albeit not significant at the 95% confidence level) corresponds to that computed for the IRM record using the same Multi Taper Method (Fig. 4a). The $CaCO_3$ record filtered at the precession frequencies of ~4 cycles/m and ~5 cycles/m shows an amplitude modulation whose envelope has been calculated using the Hilbert transform (Fig. 4b). When compared to the IRM records filtered on the short eccentricity frequency of ~1 cycle/m, the $CaCO_3$ modulation follows the short eccentricity signal, suggesting that it represents a true record of astronomical precession, with low (high) IRM values corresponding to large (small) $CaCO_3$ modulation.

## 4. Age model

The stability of the solution of orbital motion calculation is limited by the numerical accuracy of the computation and by the chaotic behavior of the Solar system (Laskar, 1990). According to Laskar et al. (2004), the only reliable component of the astronomical solution for the Mesozoic is the $(g_2 - g_5)$ term, corresponding to the 405 kyr eccentricity period, which is in any case subject to non negligible errors of about 0.1–0.2%. This implies that a time scale based on the counting of long eccentricity cycles assumed to have a fixed periodicity of 405 kyr may have an error as large as 190 kyr in the Cenomanian (Laskar et al., 2004).

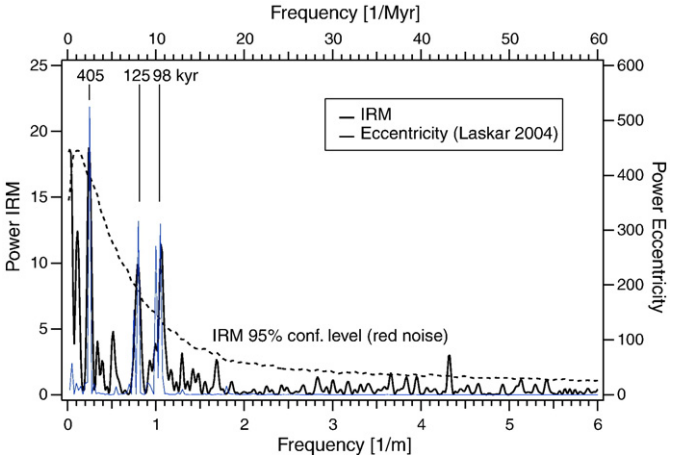


**Fig. 3.** Normalized Lomb's periodograms (Press et al., 2002) of the IRM intensity plotted versus 1/depth in the lower horizontal axis, and of orbital eccentricity from the Laskar et al. (2004) solution for the period 93–96 Myr, plotted versus 1/age in the upper horizontal axis. Horizontal axes are rescaled according to a sedimentation rate of 10 m/Myr. Confidence level for IRM (dashed line) was calculated, based on a red-noise hypothesis, according to the method proposed by Allen and Smith (1996).

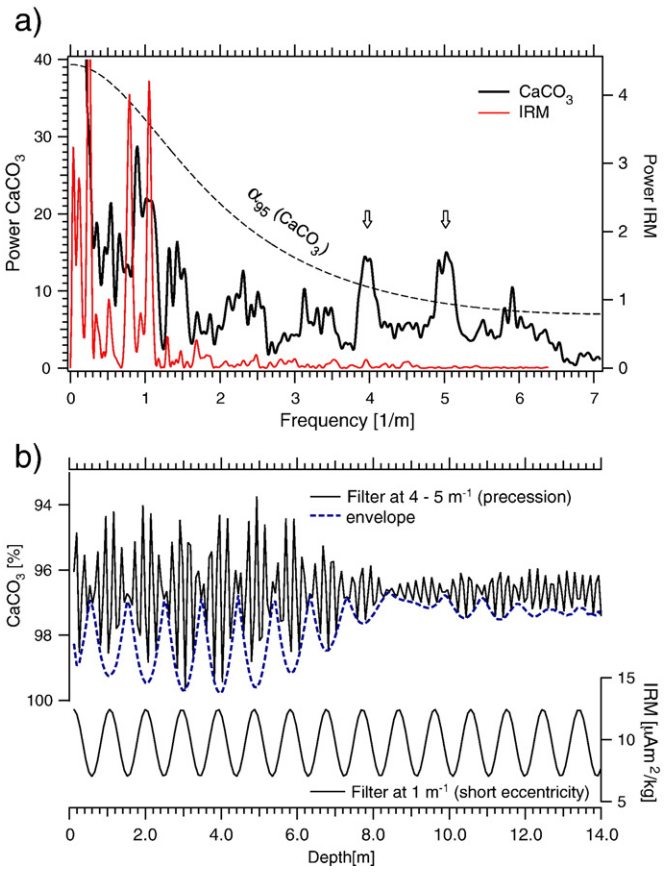


**Fig. 4.** a) Multi Taper Method power spectra of $CaCO_3$, in the upper 14 m of Furlo section, and of IRM for direct comparison. The 95% confidence level (dashed line) refers to $CaCO_3$ spectra. Periodicities corresponding to astronomical precession (arrows) are statistically significant, while the peak corresponding to the short eccentricity has a marginal significance, however it has a similar frequency of the highly significant IRM peak. b) $CaCO_3$ signal filtered at the frequencies of 4 cycles/m and 5 cycles/m, corresponding to precession, and its "envelope" showing the amplitude modulation, calculated using the Hilbert transform. In the lower panel the calcium carbonate signal is compared with IRM filtered at 1 cycle/m frequency (i.e. short eccentricity). The maxima of the filtered IRM correspond to larger amplitude modulation of the precessional signal of $CaCO_3$ which are expected during eccentricity maxima, hence IRM maxima correspond to periods of eccentricity maxima.

Based on these premises, we performed the astronomical tuning of the Furlo sequence by comparing the 405 kyr-long eccentricity cycle, from the Laskar et al. (2004) solution, with the IRM intensity filtered at the highly significant 0.25 cycle/m frequency (i.e., 4 m period) peak using the Multi Taper Method (Mann and Lees, 1996). The correct phase relationship between the IRM and the 405 kyr eccentricity cycle was established using changes in the amplitude of the precessional signal derived from the $CaCO_3$ record. The modulation of the $CaCO_3$ filtered at ~4 and ~5 cycles/m, indicates periods of eccentricity maxima, where the modulation is largest, and periods of eccentricity minima, where the modulation is nearly zero. Periods of eccentricity maxima are found to correspond to periods with larger IRM values (Fig. 4b). Conversely, periods with lower IRM value correspond to minimal orbital eccentricity.

As a radiometric tie point for our tuning, we adopted the age of ~94.1 Ma for the base of the $\delta^{13}C_{org}$ positive excursion in the Pueblo Cenomanian–Turonian boundary stratotype that Sageman et al. (2006) connected by cycle counting to radiometric dates from Obradovich

(1993). This radiometric date from Pueblo section was successfully correlated with the $\delta^{13}C_{org}$ positive excursion observed in the Furlo section at the base of the Bonarelli Level (Tsikos et al., 2004; Mort et al., 2007). Based on the above, we correlate the IRM minimum found at the base of the Bonarelli Level, which corresponds to the base of $\delta^{13}C_{org}$ excursion, with the long eccentricity minimum that is closest in age (93.95 Ma) to the age of ~94.1 Ma (Fig. 5). The preceding 5 minima in the 0.25 cycle/m (i.e., 4 m period) filtered IRM signal follow consistently the 405 kyr eccentricity cycles by simply assuming a nearly constant sedimentation rate of about 10 m/Myr, which is a reasonable assumption given the lithologically homogenous nature of the Scaglia Bianca Fm. Since the IRM spectrum exhibits large power corresponding to the short eccentricity frequency bands, it is also possible to compare the full eccentricity solution of Laskar et al. (2004) with the IRM intensity filtered at peaks of 1.0 cycle/m, 0.8 cycle/m and 0.25 cycle/m as well as with the unfiltered IRM intensity (Fig. 5). Interestingly, also the short period (1 to 1.25 m) IRM variations appear to be in phase with the orbital solution (Laskar et al., 2004), which might suggest that the calculations for these components are correct. Based on the above correlation, the 20 m-thick interval comprised between the section base and the base of the Bonarelli Level spans ~2.1 Myr (Fig. 5) with an average sedimentation rate of ~10 m/Myr in agreement with previous astronomical calibration (Mitchell et al., 2008). Finer scale variations in sedimentation rate throughout the section can be calculated by taking into account the thickness of individual short eccentricity cycles (1 to 1.25 m) in the IRM record. This exercise is independent from the precision of the astronomical calculation for these components since their period is not expected to change significantly. The resulting sedimentation rate (Fig. 6a) shows an average of 9.9 m/Myr and long period (~4 m) changes synchronous with IRM fluctuation, hence eccentricity, with high sedimentation rates corresponding to low eccentricity periods.

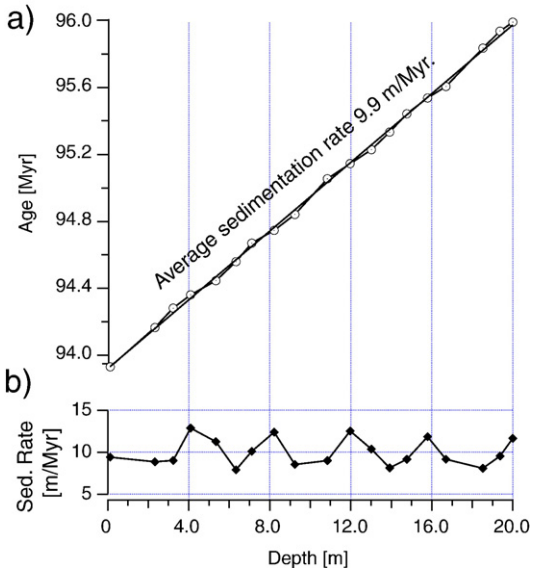


**Fig. 6.** Sedimentation rate of the Cenomanian Scaglia Bianca based on the astronomical tuning of the short eccentricity cycles. Although the average sedimentation rate appears rather constant (a), there are significant long-term variations with a period of 4 m (b), which corresponds to the long eccentricity cycle (405 kyr).

## 5. Discussion

The magnetic properties of the upper Cenomanian Scaglia Bianca Fm. at Furlo show a remarkably clear rhythmic pattern that is related to Earth's eccentricity. In particular, we were able to directly isolate the term $(g_2 - g_5)$, with a period of 405 kyr, which has a stable numerical solution for the Mesozoic era (Laskar et al., 2004). The direct phase relationship between the eccentricity signal and the IRM intensity is deduced from the amplitude modulation of the precessional signal recorded in the calcium carbonate record. We found that the amplitude of the precession-related signal is modulated by the short (~100 kyr) eccentricity and shows larger variability in correspondence of the IRM maxima that, by implication, correspond to maximal orbital forcing modulation. On this basis, we tuned IRM maxima with maxima of eccentricity and IRM minima with eccentricity minima. Accordingly, within the ~2.1 Myr-long time interval preceding the onset of the Bonarelli Level black shales and/or black cherts (as proxied by IRM minima) preferentially deposited during ~100 kyr eccentricity minima within 405 kyr minima (Fig. 5).

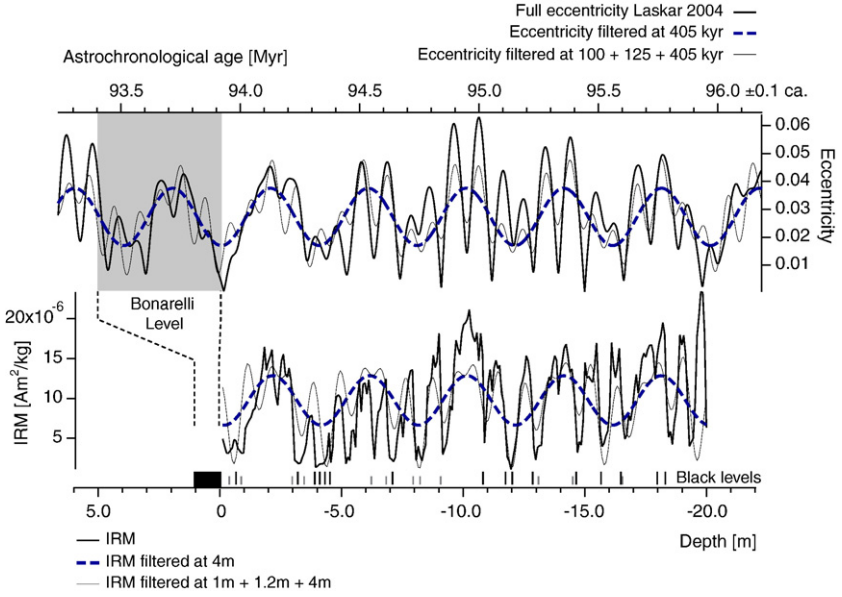


**Fig. 5.** Tuning of the IRM signal to the astronomical solution of Laskar et al. (2004). The IRM filtered at 4 m period was tuned to the corresponding 405 kyr-filtered eccentricity by assuming a constant sedimentation rate of 10 m/Myr (see text for details). The IRM minimum at the top of the section was linked to the 405 kyr minimum closest to the estimated age of 94.1 Myr for the base of Bonarelli Level. The IRM and the eccentricity filtered on the main spectral peaks of 1 m, 1.2 m, 4 m and 100 kyr, 125 kyr, 405 kyr respectively, compare well and allow a finer tuning based using the short eccentricity cycles. The position of black shales (tall black), black chert (low grey), the Bonarelli Level and their correlation with astronomical eccentricity is also shown. A duration of the Bonarelli Level of ~500 kyr is assumed according to Mort et al. (2007).

Recently, Mitchell et al. (2008) attempted to correlate the rhythmic lithological properties of the Cenomanian Scaglia Bianca Fm. at Furlo with the astronomical solution of Laskar et al. (2004), using a facies rank-depth method. Their cyclostratigraphic results are broadly similar to those presented in this study in terms of cycle counting, albeit the stable Mesozoic eccentricity term (405 kyr) was indirectly derived from the precession envelope assumed to represent the complete eccentricity signal. Their tuning was achieved starting from the same initial tie point of ~94.1 Ma for the base of the Bonarelli Level and searching for the best peak and amplitude matching between the precession-derived short eccentricity signal, which they found in the Scaglia Bianca Fm. depth-rank series, and the full eccentricity solution from Laskar et al. (2004). The resulting correlation implied a systematic coincidence between eccentricity maxima and black shale levels, which they explained by invoking the monsoonal model developed for the Pliocene–Pleistocene Mediterranean sapropels. In their preferred interpretation, the onset of the Bonarelli Level is placed at 94.21 Ma within a long eccentricity maximum, and the level itself persisted over a protracted period (340 kyr) of unusually low insolation variability (eccentricity and obliquity) due to a simultaneous node in all orbital parameters of the astronomical solution. Based on this coincidence, Mitchell et al. (2008) hypothesized that the timing of the Bonarelli Level as well as other OAEs are controlled by very long-term (~2.45 Myr) astronomical variations. However, since the only astronomical parameter that can be reliably computed for the Mesozoic is the $(g_2-g_5)$ term (Laskar et al., 2004) and the age of the other eccentricity terms is subject to a large uncertainty, the actual age of such nodes cannot be determined. Although attractive, the correlation of the Bonarelli Level (and possibly other OAEs) with the peculiar orbital configuration proposed by Mitchell et al. (2008) cannot be established at present because the chaotic evolution of the orbits prevents a precise determination of the Earth's motion, and astronomical calculation for periods older than about 60 Ma does not have the desirable precision.

Given the possible errors (up to 190 kyr) associated with the astronomical calculations for the Cenomanian, and considering that these intrinsic errors sum up to errors associated with the correlations and with the radiometric ages, the main practical difference between the age model of Mitchell et al. (2008) and ours is the opposite phase relationship of the 405 kyr eccentricity term. In fact, our successful determination of the phase relationship between the geologic record and the astronomical solution clarifies the orbital configuration that led to the formation of black shales, as well as magnetite dissolution, and confirms previous assertions that mid-Cretaceous rhythmic black shales formed during periods of eccentricity minima. In particular, our findings accredit the anti-monsoonal model of black shales formation previously proposed by Herbert and Fischer (1986) for the Aptian–Albian Marne a Fucoidi Formation.

The scrutiny of the sedimentation rate (Fig. 6b) shows significant long-term variations with a period virtually identical to the long eccentricity but with opposite phase (i.e., higher sedimentation rates corresponding to long eccentricity minima), which is corroborated by the analysis of calcium carbonate content showing the same opposite phase relationship. These variations are difficult to explain as a consequence of $CaCO_3$ productivity because the oligotrophic conditions occurring during periods of eccentricity minima, as inferred from nannofossil and foraminiferal records (Premoli Silva et al., 1989; Galeotti, 1998) and predicted by the anti-monsoonal model (Herbert and Fischer, 1986), would favor a decrease of nutrient recycling. We infer that the main factor controlling the variability of the sedimentation rate in the Cenomanian Scaglia Bianca Formation is likely to be the preservation of $CaCO_3$. Kuhnt et al. (2009) reported Cenomanian sea-level fluctuations that were paced by the long eccentricity (405 kyr) with low-stands associated with eccentricity minima. We speculate that an increase of ocean water alkalinity related to the suppression of shallow water carbonate production during low-stands could have enhanced $CaCO_3$ preservation in these periods providing a plausible mechanism to explain the observed variability of sedimentation rate.

## 6. Conclusions

Spectral analysis of rock-magnetic properties of the Scaglia Bianca Fm. at Furlo and its phase relationships with the astronomical solution for the late Cenomanian, show evidence that black shales deposition and the onset of the Bonarelli Level occurred during times of eccentricity minima as predicted by the anti-monsoonal model of Herbert and Fischer (1986). In line with this model, the onset of the Bonarelli Level deposition and the associated $\delta^{13}C_{org}$ perturbation fall in correspondence of an eccentricity minimum, as in the case of the preceding black shales. With the orbitally controlled series of $C_{org}$-rich deposits, however, the Bonarelli Level obviously represents a much larger event in terms of magnitude and duration as it persisted across at least one long eccentricity maximum. Whether or not this and other Cretaceous OAEs are paced by very long-term eccentricity variations, as proposed by Mitchell et al. (2008), cannot be established by direct comparison with the full astronomical solution because of its insufficient precision. However, it could in principle be tested by astronomically tuning the time elapsed between several OAEs using the reliable $(g_2-g_5)$ term.

We notice that the IRM short (~100 kyr) eccentricity cycles appear to be in phase with the solution of Laskar et al. (2004) suggesting a positive test for the accuracy of this component. Fine-tuning of the IRM record revealed a cyclic variation of sedimentation rate that increases during period of eccentricity minima and black shales deposition. The observed periodicity of the sedimentation rate, of about 400 kyr, was related to orbitally controlled sea-level fluctuations (Kuhnt et al., 2009) and explained as enhanced carbonate preservation during low-stand periods. According to this scenario, black shales formed probably because of reduced oceanic mixing, deep-water formation, and sea bottom ventilation that promoted organic matter preservation. Conditions of reduced deep-water formation were preferentially achieved during periods of low orbital eccentricity when the insolation variability due to precession was reduced, seasonality and monsoonality dumped (e.g., Herbert and Fischer, 1986; Premoli Silva et al., 1989; Herbert and D'Hondt, 1990; Erba, 1992; Galeotti et al., 2003) and sea level was at low-stand (Kuhnt et al., 2009). These conjunctures may have put the Alpine Tethys–Central Atlantic Ocean, which was a relatively constricted basin with narrow or morphologically complex connections with the Pacific and South Atlantic Oceans, in a metastable state with respect to deep-water circulation that was susceptible to small external forcing, especially if the source of high latitude (cooler and better oxygenated) deep water was located in the Southern Ocean (Poulsen et al., 2001).

## Acknowledgments

We are deeply in debt with Simone Galeotti for countless advices and the many discussions that helped improve this manuscript. The paper benefited from the review of Ross Mitchell and other three anonymous reviewers.

## References

Allen, M., Smith, L.A., 1996. Monte Carlo SSA: detecting irregular oscillations in the presence of coloured noise. J. Climatol. 9, 3373–3404.
Arthur, M.A., Premoli Silva, I., 1982. Development of widespread organic carbon-rich strata in the Mediterranean Tethys. In: Schlanger, S.O., Cita, M.B. (Eds.), Nature and Origin of Cretaceous Carbon-Rich Facies. Academic Press, London, pp. 7–54.
Arthur, M.A., Brumsack, H.-J., Jenkyns, H.C., Schlanger, S.O., 1990. Stratigraphy, geochemistry, and paleoceanography of organic carbon-rich Cretaceous sequences. In: K.A. Publ. (Editor), Cretaceous Resources, Events, and Rhythms, pp. 75–119.
Bralower, T.J., Zachos, C.J., Thomas, E., Parrow, M., Paull, C.K., Premoli Silva, I., Sliter, W.V., Lohmann, K.C., 1995. Late Paleocene to Eocene paleoceanography of the equatorial Pacific Ocean: stable isotopes recorded at Ocean Drilling Program Site 865, Allison Guyot. Paleoceanography 10 (4), 841–865.
Coccioni, R., Galeotti, S., 2003. The mid-Cenomanian Event: prelude to OAE 2. Palaeogeogr., Palaeoclimatol., Palaeoecol. 190 (14), 427–440.
Dunlop, D.J., Ozdemir, O., 1997. Rock Magnetism: Fundamentals and Frontiers. Cambridge University Press, Cambridge. 573 pp.
Emeis, K.-C., Weissert, H., 2009. Tethyan–Mediterranean organic carbon-rich sediments from Mesozoic black shales to sapropels. Sedimentology 56 (1), 247–266.

Erba, E., 1992. Calcareous nannofossil distribution in pelagic rhythmic sediments (Aptian–Albian Piobbico core, Central Italy). Riv. Ital. Paleontol. Stratigr. 97, 455–484.
Galeotti, S., 1998. Planktic and benthic foraminiferal distribution patterns as a response to changes in surface fertility and ocean circulation: a case study from the Late Albian 'Amadeus Segment' (Central Italy). J. Micropaleonlogy 17 (1), 87–96.
Galeotti, S., Sprovieri, M., Coccioni, R., Bellanca, A., Neri, R., 2003. Orbitally modulated black shale deposition in the upper Albian Amadeus Segment (central Italy): a multi-proxy reconstruction. Palaeogeogr., Palaeoclimatol., Palaeoecol. 190, 441–458.
Galeotti, S., Rusciadelli, G., Sprovieri, M., Lanci, L., Gaudio, A., Pekar, S., 2009. Sea-level control on facies architecture in the Cenomanian–Coniacian Apulian Margin (western Tethys): a record of glacioeustatic fluctuations during the Cretaceous greenhouse? Palaeogeogr., Palaeoclimatol., Palaeoecol. 276 (1–4), 196–205.
Gradstein, F.M., Ogg, J.G., Smith, A.G., Agterberg, F.P., Bleeker, W., Cooper, R.A., Davydov, V., Gibbard, P., Hinnov, L., House, M.R., Lourens, L., Luterbacher, H.-P., McArthur, J., Melchin, M.J., Robb, L.J., Shergold, J., Villeneuve, M., Wardlaw, B.R., Ali, J.R., Brinkhuis, H., Hilgen, F.J., Hooker, J., Howarth, R.J., Knoll, A.H., Laskar, J., Monechi, S., Powell, J., Plumb, K.A., Raffi, I., Röhl, U., Sanfilippo, A., Schmitz, B., Shackleton, N.J., Shields, G.A., Strauss, H., Van Dam, J., Veizer, J., van Kolfschoten, T., Wilson, D., 2004. A Geologic Time Scale 2004. Cambridge University Press.
Herbert, D.T., D'Hondt, L.S., 1990. Precessional climate cyclicity in Late Cretaceous–Early Tertiary marine sediments: a high resolution chronometer of Cretaceous–Tertiary boundary events. Earth Planet. Sci. Lett. 99 (3), 263–276.
Herbert, T.D., Fischer, A.G., 1986. Milankovitch climatic origin of mid-Cretaceous black shale rhythms in central Italy. Nature 321, 739–743.
Hilgen, F.J., 1991a. Extension of the astronomically calibrated (polarity) time scale to the Miocene/Pliocene boundary. Earth Planet. Sci. Lett. 107, 349–368.
Hilgen, F.J., 1991b. Astronomical calibration of Gauss to Matuyama sapropels in the Mediterranean and implication for the geomagnetic polarity time scale. Earth Planet. Sci. Lett. 104, 226–244.
Hilgen, F.J., Krijgsman, W., Langereis, C.G., Lourens, L.J., Santarelli, A., Zachariasse, W.J., 1995. Extending the astronomical (polarity) time scale into the Miocene. Earth Planet. Sci. Lett. 136, 495–510.
Kuhnt, W., Holbourn, A., Gale, A., Chellai, E.H., Kennedy, W.J., 2009. Basin (SW Morocco) Cenomanian sequence stratigraphy and sea-level fluctuations in the Tarfaya. Geol. Soc. Am. Bull. 121, 1695–1710.
Kuroda, J., Ohkouchi, N., Ishii, T., Tokuyama, H., Asahiko, T., 2007. Lamina-scale analysis of sedimentary components in Cretaceous black shales by chemical compositional mapping: implications for paleoenvironmental changes during the Oceanic Anoxic Events. Geochim. Cosmochim. Acta 69 (6), 1479–1494.
Laskar, J., 1990. The chaotic motion of the Solar System: a numerical estimate of the size of the chaotic zones. Icarus 88, 266–291.
Laskar, J., Robutel, P., Joutel, F., Gastineau, M., Correia, A.C.M., Levrard, B., 2004. A long-term numerical solution for the insolation quantities of the Earth. Astron. Astrophys. 428, 261–285.
Lowrie, W., Alvarez, W., 1984. Lower Cretaceous magntic stratigraphy in Umbrian pelagic limestone sections. Earth Planet. Sci. Lett. 71, 315–328.
Lowrie, W., Alvarez, W., Premoli Silva, I., Monechi, S., 1980. Lower Cretaceous magnetic stratigraphy in Umbrian pelagic carbonate rocks. Geophys. J. R. Astronom. Soc. 60, 263–281.
Mann, M.E., Lees, J., 1996. Robust estimation of background noise and signal detection in climatic time series. Clim. Change 33, 409–445.
Mitchell, R.N., Bice, D.M., Montanari, A., Cleaveland, L.C., Christianson, K.T., Coccioni, R., Hinnov, A.L., 2008. Oceanic anoxic cycles? Orbital prelude to the Bonarelli Level (OAE 2). Earth Planet. Sci. Lett. 26, 1–16.
Mort, H., Jacquat, O., Adatte, T., Steinmann, P., Fölmi, K., Matera, V., Berner, Z., Stüben, D., 2007. The Cenomanian/Turonian anoxic event at the Bonarelli Level in Italy and Spain: enhanced productivity and/or better preservation? Cretaceous Res. 28, 597–612.
Obradovich, J.D., 1993. A Cretaceous time scale. In: Caldwell, W.G.E., Kauffman, E.G. (Eds.), Evolution of the Western Interior Basin: Geological Association of Canada Special Paper, pp. 379–396.
Poulsen, C.J., Barron, E.J., Arthur, M.A., Peterson, W.H., 2001. Response of the mid-Cretaceous global oceanic circulation to tectonic and $CO_2$ forcing. Paleoceanography 16 (6), 576–592.
Premoli Silva, I., Erba, E., Tornaghi, M.E., 1989. Paleoenvironmental signals and changes in surface fertility in mid Cretaceous $C_{org}$-rich pelagic facies on the Fucoid Marls (central Italy). Geobios Mem. Spec. 11, 225–236.
Press, H.W., Teukolsky, A.S., Vetterling, T.W., Flannery, P.B., 2002. Numerical Recipes in C: The Art of Scientific Computing, 2nd Ed. Cambridge University Press, Cambridge.
Rohling, E.J., Hilgen, F.J., 1991. The eastern Mediterranean climate at times of sapropel formation: a review. Geol. Mijnbouw 70, 253–264.
Rossignol-Strick, M., 1985. Mediterranean quaternary sapropels, an immediate resonse of the African monsoon to variation of insolation. Palaeogeogr., Palaeoclimatol., Palaeoecol. 49, 237–263.
Sageman, B.B., Meyers, R.S., Arthur, A.M., 2006. Orbital time scale and new C-isotope record for Cenomanian–Turonian boundary stratotype. Geology 34 (2), 125–128. doi:10.1130/G22074.1.
Tsikos, H., Jenkyns, H.C., Walsworth-Bell, B., Petrizzo, M.R., Forster, A., Kolonic, S., Erba, E., Premoli Silva, I., Baas, M., Wagner, T., Sinninghe Damste, J.S., 2004. Carbon-isotope stratigraphy recorded by the Cenomanian–Turonian Oceanic Anoxic Event: correlation and implications based on three key localities. J. Geol. Soc. 161 (4), 711–719. doi:10.1144/0016-764903-077.
Voigt, S., Aurag, A., Leis, F., Kaplan, U., 2007. Late Cenomanian to Middle Turonian high-resolution carbon isotope stratigraphy: new data from the Münsterland Cretaceous Basin, Germany. Earth Planet. Sci. Lett. 253 (1–2), 196–210.